Energy Engineering

Tech Science Press

Doi:10.32604/ee.2025.063268

REVIEW

A Review on the Research Progress of Layered Double Hydroxides Electrode Materials for Supercapacitors

Hengzheng Li[1,2] **and Jie Yang**[1,*]

[1]School of Mechanical and Electronic Engineering, Suzhou University, Suzhou, 234000, China
[2]School of Chemistry and Materials Science, University of Science and Technology of China, Hefei, 230026, China

*Corresponding Author: Jie Yang. Email: yanger@ahszu.edu.cn

Received: 10 January 2025; Accepted: 26 March 2025; Published: 27 June 2025

ABSTRACT: Layered double hydroxides (LDHs) are a class of transition metal-based materials characterized by their two-dimensional nano-layered structure. They offer several advantages, such as easy adjustability of morphology and structure and simple preparation methods, making them highly promising for the development of low-cost, high energy density supercapacitors. This article begins with a brief introduction to the basic structure, energy storage mechanism, and application challenges of LDHs. It then proceeds to summarize the innovations in the preparation methods of LDH electrode materials, such as the application of high precision synthesis technologies including component regulation, amorphization, and the introduction of oxygen vacancies. The achievements in performance optimization are also analyzed, for example, the improvement of specific capacitance and rate performance through nanostructure design and nanosizing treatment. However, it is also pointed out that there are problems such as low charge transfer efficiency and poor cycling stability in practical applications. This review is of great reference value for a deep understanding of the research status and development direction of LDH electrode materials. It is expected that breakthroughs will be achieved in aspects such as green and sustainable preparation processes and the expansion of applications in multiple fields in the future.

KEYWORDS: LDHs; supercapacitors; the intrinsic reactivity; specific surface area; electronic transmission

1 Introduction

Supercapacitors have notable advantages in power density, charging and discharging speed, and service life, and have been rapidly developed in the fields of power and automation [1–3]. However, their relatively low energy density [4,5] limits their application in important fields such as electric vehicles and portable devices [6,7]. Therefore, researching and designing new electrode materials is of great significance for enhancing the energy density of supercapacitors and expanding their applications. As shown in the capacitor's energy equation:

$$E = 1/2\,CV^2 \tag{1}$$

where V represents the working voltage of the capacitor and C denotes its capacitance. Enhancing both V and C can boost the energy density of a capacitor. The value of V hinges on the electrolyte type. Organic electrolyte capacitors can achieve a working voltage of up to 3 V, yet they have stringent safety and operating environment requirements and involve high preparation costs [8,9]. In contrast, aqueous electrolytes, while advantageous in cost and environmental protection, are limited by the water decomposition voltage, so

Copyright © 2025 The Authors. Published by Tech Science Press.
This work is licensed under a Creative Commons Attribution 4.0 International License, which permits unrestricted use, distribution, and reproduction in any medium, provided the original work is properly cited.

the working voltage of aqueous supercapacitors generally should not exceed 1.2 V [10,11]. Therefore, there is a significant bottleneck in obtaining high energy density supercapacitors by increasing the value of V. Compared with raising the working voltage of the capacitor, increasing the value of C is a relatively simpler approach. Developing and preparing high performance electrode materials is a straightforward and effective method to boost the value of C. Inspired by this strategy, researchers have developed and studied a variety of electrode materials and achieved promising results [12–15].

There are two types of capacitors: electronic double-layer capacitors (EDLCs) and Faraday capacitors. Their working principles are distinct. EDLCs store energy through electrostatic adsorption on the electrode surface. Specific surface area (SSA) is a crucial indicator determining this capacitor's performance [16]. Carbon materials are typical EDLC materials. For instance, graphene, with a large SSA, when used as an electrode, has a theoretical specific capacitance (SC) of about 500 F/g, which offers limited potential for enhancing the capacitor's energy density [17].

The Faraday capacitor, or pseudo capacitor, relies on fast and reversible redox reactions to store and release charges, thereby achieving capacitance. Transition metal-based materials are typical for this type of capacitor. These electrode materials have a high theoretical capacity, with maximum SC values exceeding 1000 F/g [18]. However, electrodes made from transition metal-based materials commonly suffer from poor conductivity and rate capability, which restrict their overall performance.

LDHs are a class of transition metal-based materials with a two-dimensional nano layered structure. They boast easily adjustable morphology and structure, low cost, and simple preparation methods, making them promising candidates for achieving low cost, high-energy density supercapacitors [3,4,19]. However, due to their low intrinsic activity and high charge transfer resistance, the actual capacitance performance of LDHs falls short of their theoretical values, failing to meet practical demands. For instance, the theoretical SC of Ni-Co-LDH can reach 3000 F/g [20], but samples prepared via traditional methods typically exhibit SC values below 1000 F/g. Even after special treatment, while Ni-Co-LDH samples can achieve over 2000 F/g, there remains a significant gap compared to their theoretical potential [21,22]. To address these limitations and enhance the reactivity and charge transfer efficiency of LDHs, researchers have explored various improvement strategies in recent years, achieving remarkable progress.

This article begins by outlining the fundamental structure and energy storage mechanism of LDHs electrode materials, and delves into the issues and challenges they face in energy storage applications. Subsequently, it encapsulates the efforts and explorations to enhance the energy storage performance of LDH electrode materials from three perspectives: boosting the intrinsic reaction activity and SSA of the materials, and expediting the charge transfer kinetics. Detailed coverage is provided on multiple approaches, including component regulation, the construction of hierarchical structures, and compounding with conductive materials. Finally, it proposes four potential research directions for LDH electrode materials. The work presented in this article may serve as a reference for readers to swiftly grasp the development and practical applications of LDH electrode materials in energy storage.

2 Overview of LDHs

2.1 Structure of LDHs

LDHs are a two-dimensional nano-layered material primarily consisting of positively charged hydroxide layers. Anions and water molecules are present between these layers [22,23]. Within this structure, ionic bonds connect the interior of the layers, while hydrogen bonding and electrostatic interactions bond the

layers to the anions. The anions serve as spacers between the LDH layers and neutralize the positive charge of the hydroxide layers. The general chemical formula for LDHs is:

$$\left[M_{1-x}^{2+}\ M_{x}^{3+}\ (OH)_2\right]^{x+}\left[A_{x/n}^{n-}\right]^{x-}\cdot mH_2O \tag{2}$$

where M^{3+} represents a trivalent metal cation, such as Al^{3+}, Fe^{3+}, Co^{3+}, Cr^{3+}, etc. M^{2+} represents a divalent metal cation, such as Co^{2+}, Ni^{2+}, Cu^{2+}, Co^{2+}, Mg^{2+}, Zn^{2+}, etc. A^{n-} represents the interlayer anion, such as NO_3^-, Br^-, CO_3^{2-}, NO_3^-, SO_4^{2-}, Cl^- etc. m represents the amount of crystalline water. The value of x in the general formula directly affects the composition of the product, and changes in the value can affect the structure of the compound and even generate other products. In the general formula, the value of x directly affects the product's composition and the compound's structure [5]. Fig. 1 presents the structural model of LDHs.

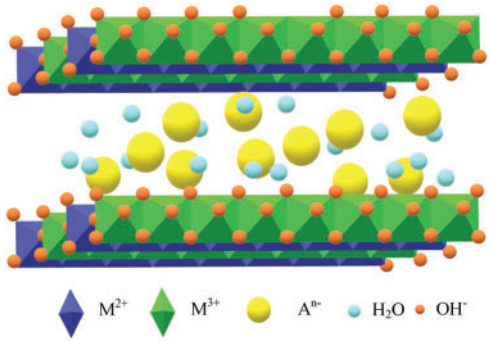

Figure 1: The structure model of LDHs

2.2 Energy Storage Mechanism of LDHs

In alkaline electrolytes, LDHs primarily store energy via the interplay of divalent and trivalent transition metal cations. During charging and discharging, the metal hydroxide within the layers undergoes a reversible redox reaction to store and release charges. When charging, electrons mainly move along the layers, with a few moving across them. Electrolyte ions transport and diffuse through the gaps in the layers. Take the Ni-Co-LDH electrode as an example. During charging, the metal hydroxide loses an electron, and the OH group on the layer loses a H^+ to form an H vacancy (H_v). The connected nickel/cobalt changes from divalent to trivalent, forming hydroxyl oxides. The released H^+ combines with OH^- in the electrolyte to form H_2O. Some hydroxyl cobalt oxide converts to cobalt dioxide, enhancing the theoretical SC [24]. During discharging, the hydroxyl oxide gains an electron, the H vacancy on the layer combines with H^+ from the electrolyte, and the connected nickel/cobalt reverts to divalent, returning to its original state.

2.3 Challenges Faced by LDHs

As previously stated, the capacitive performance of LDHs stems from reversible redox reactions occurring on their surfaces. Consequently, the intrinsic reactivity, SSA, and charge transfer dynamics of LDHs play a pivotal role in influencing their capacitive performance. A high intrinsic reactivity and an elevated SSA are capable of enhancing the intensity of the reversible redox reactions taking place on the surface of the LDHs electrode, thereby improving its energy storage performance. Conversely, lower levels of these parameters will restrict its energy storage capabilities [25,26].

During practical electrode use, superior electron and ion transfer dynamics at the redox interface lead to lower electrode voltage drops and higher specific capacities under high current densities. LDHs have a great layered structure with rich active sites and remarkable theoretical capacity for electrochemical energy storage [27–31]. However, in practical use, they face issues like low intrinsic reactivity, poor conductivity, easy agglomeration, and slow interlayer ion diffusion. Properly solving these problems is crucial for developing high-performance LDH-based electrodes and supercapacitors.

To address the challenges of LDHs materials in supercapacitors, researchers have extensively studied and explored ways to enhance their energy storage performance. Based on different strategies, these efforts can be categorized into three main aspects: improving intrinsic reaction activity, increasing SSA, and enhancing charge transfer kinetics [32–35]. Boosting intrinsic reaction activity and SSA can lower the critical point of reversible redox reactions, while improving charge transfer dynamics benefits electron and ion transport in supercapacitors.

Currently, common methods to enhance the intrinsic reaction activity of LDHs include component regulation, amorphization, and oxygen vacancy introduction. Increasing the active SSA allows more active sites per unit size, with common approaches being nano-materialization and hierarchical structure construction. Improving charge transfer dynamics can be achieved by enhancing conductivity and ion transfer channels. Better electrode conductivity aids electron transport during redox reactions, and this can be done by preparing composite electrodes with good conductors or directly making integral electrodes on conductive substrates. Improving ion transport channels increases electrolyte mass transfer efficiency, often through methods like expanding and adjusting material interlayer spacing.

3 Enhancing the Intrinsic Reactivity of Materials

3.1 Component Regulation

Composition control of LDHs involves adjusting the type and proportion of metals in the main layer or doping with other elements. This is a quick and effective way to enhance the storage performance of LDHs. Different metal elements have different reactivities. Changing the metal composition of LDHs can improve their intrinsic reactivity and thus achieve better capacitive performance. For example, LDHs materials prepared using pure Ni, Fe, Al, etc., typically have a SC value below 1500 F/g [36], whereas those made from a combination of Ni and Co can achieve an SC value exceeding 2000 F/g [21].

Maintaining the metal composition in the primary layer of LDHs while suitably adjusting the atomic ratio can enhance the material's micro-morphology, crystal structure, and intrinsic reactivity. Wei et al. [37] fabricated dispersed Ni-Co-LDHs ultrathin nanosheets on a nickel foam substrate through controlled electrodeposition. They optimized the surface structure and capacitance by varying the $Ni(OAc)_2/Co(NO_3)_2$ molar ratio. The material achieved a specific capacitance of 1587.5 F/g at 0.5 A/g with good rate and cycle stability when the ratio was 0.64/0.36. Xie et al. [5] prepared CoxNi1-x-LDHs with different Ni/Co ratios via chemical coprecipitation using polypropylene pyrrolidone. Their results indicated that the sample with x = 0.57 exhibited high reactivity, reaching a specific capacitance of 2614 F/g, and retained 86.4% of its capacity after 1000 cycles at 5 A/g.

The ternary composite material formed by doping trivalent transition metal ions into LDHs can enhance the crystallinity of the laminates, improve reactivity, and increase the SC value. Wang et al. [36] synthesized Ni-Co-Al-LDH by incorporating Al^{3+} into Ni-Co-LDHs. The doped Al^{3+} enhances the crystallinity and reactivity of Ni-Co-LDHs, resulting in an SC value of 2062 F/g at 1 A/g for Ni-Co-Al-LDHs. Fig. 2 presents the XRD patterns, FESEM, and TEM images of Ni-Co-Al-LDH. Xiong et al. [38] prepared Ni-Co-Mn-LDHs by introducing Mn^{3+} during the synthesis of Ni-Co-LDHs. Fig. 3 shows the morphology and characterization

results of Ni-Co-Mn-LDHs. Research indicates that Mn^{3+} addition significantly improves the capacitive properties, rate capability, and cycle life compared to Ni-Co-LDHs. Wang et al. [39] developed P@NiCo-LDH composite electrode materials via low-temperature coprecipitation followed by phosphating annealing, and investigated the differences between phosphated and unphosphated Ni-Co-LDHs. Initially, single-crystalline Ni-Co-LDH nanomaterials with cabbage-like nanospheres were synthesized via low-temperature coprecipitation. Subsequently, P@NiCo-LDH electrode materials were obtained through phosphating and annealing. Results show that P@NiCo-LDHs exhibit an SC value of 1340 F/g at 1 A/g, which is 1.88 times higher than that of Ni-Co-LDHs.

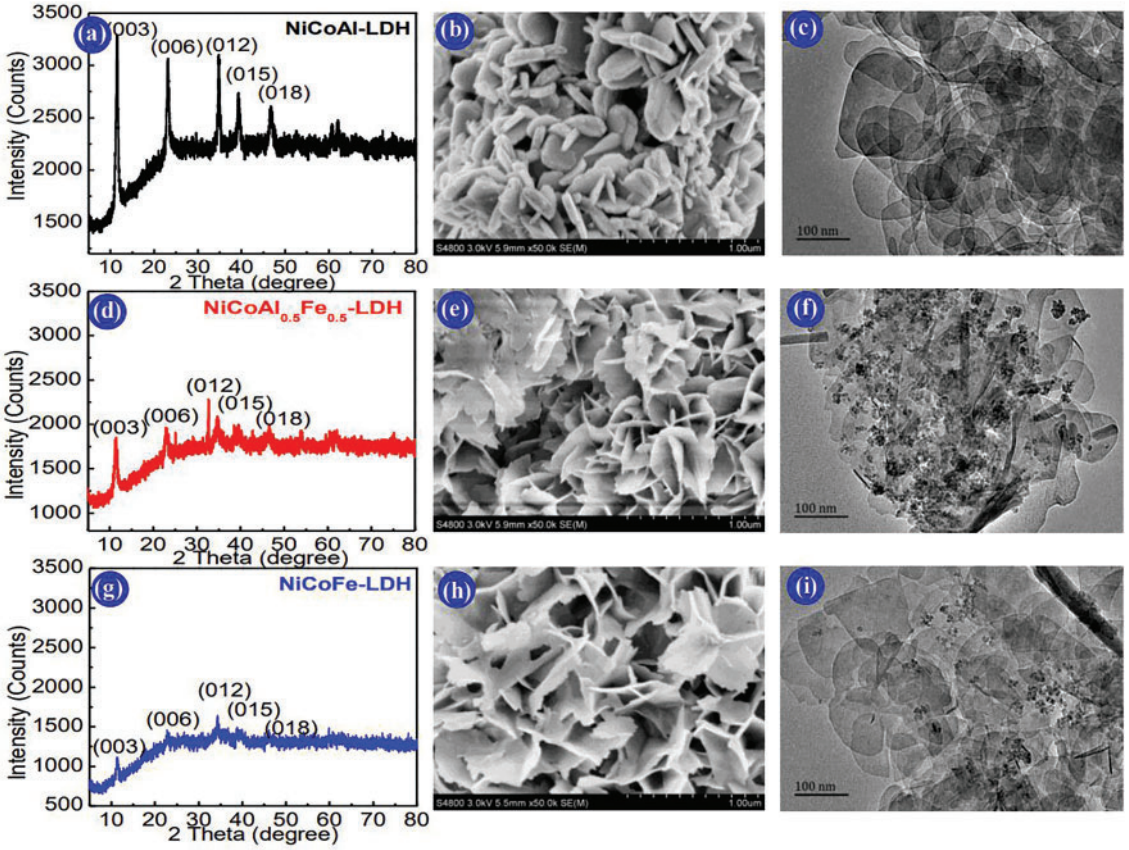

Figure 2: XRD patterns, FESEM and TEM images of the Ni-Co-Al-LDH (a–c), Ni-Co-$Al_{0.5}$-$Fe_{0.5}$-LDH (d–f) and Ni-Co-Fe-LDH (g–i) [36]

3.2 Amorphous LDH-Like Materials

Amorphous materials feature short-range order and long-range disorder in atomic or molecular arrangement, with numerous unsaturated coordination sites [40]. Leveraging these features, amorphous LDH-like analogues can be synthesized. These analogues, with a composition akin to LDHs (M^{2+}/M^{3+} bimetallic hydroxides, interlayer anions) and short-range order (e.g., local lamellar units), transcend crystal structure limitations on active sites. In supercapacitors, amorphous LDH-like materials boost electrochemical activity, energy storage, and cycling stability [6].

Chen et al. [41] used a mixed-solvent method to obtain amorphous NiCoMn-OH. Tests show it has good electrochemical activity and rate capability. The experiment also indicated that solvent mixing is crucial

for synthesizing amorphous NiCoMn-OH. Fig. 4 presents the FESEM and TEM images of the NiCoMn-OH sample. Huang et al. [42] prepared amorphous nickel-based hydroxides via hydrothermal synthesis incorporating ethylene glycol. Results show amorphous NiCo-OH has specific capacities of 888 C/g at 1 A/g and 662 C/g at 50 A/g. Yao et al. [3] used an ultrasonic-assisted reduction method to *in-situ* grow amorphous $NiFe(OH)_x$ on the surface of $NiFe_2O_4$. Tests indicate it has excellent electrochemical performance, with an overpotential of 276 mV at 10 mA/cm².

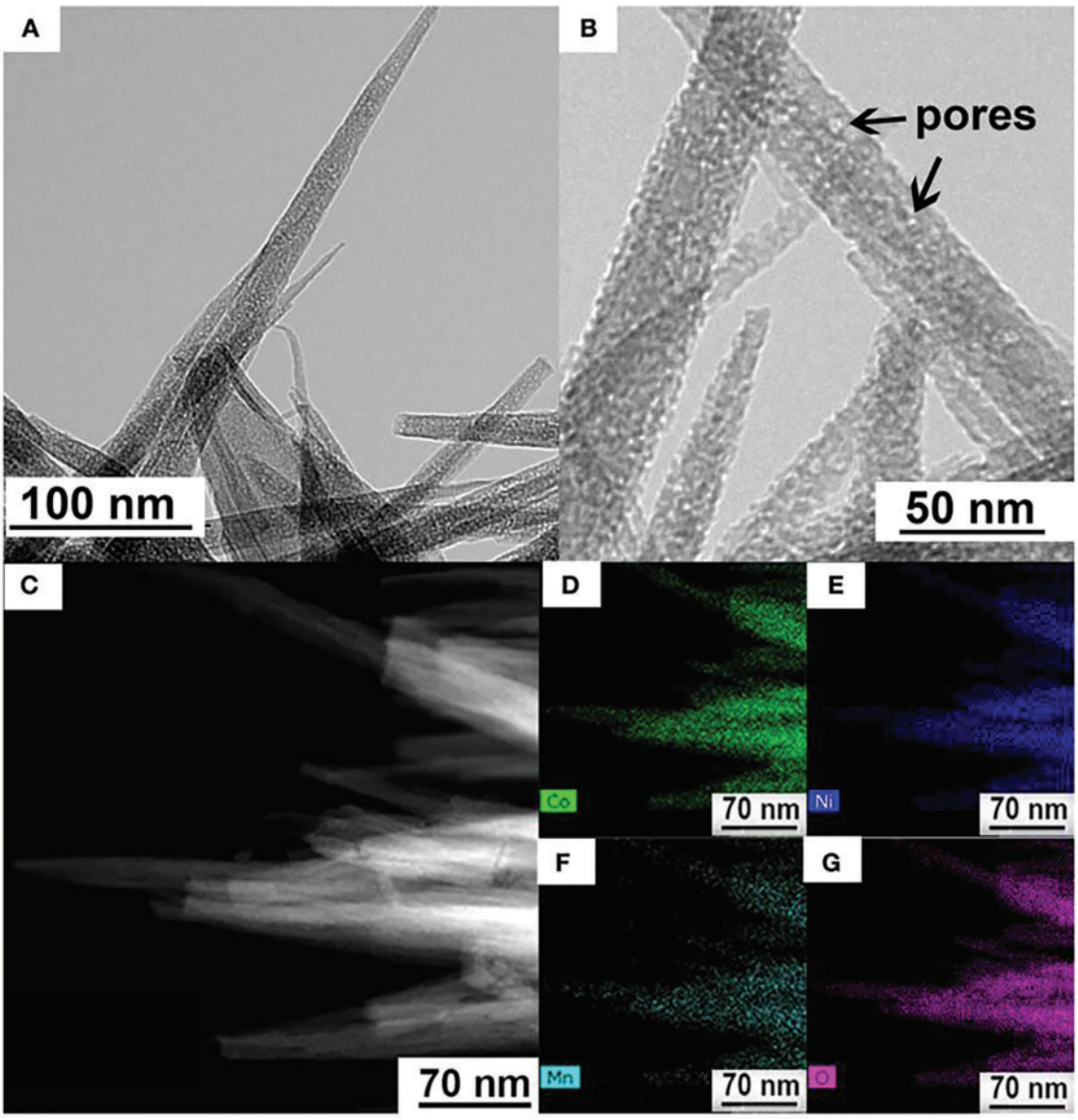

Figure 3: The morphology and characterization results of Ni-Co-Mn-LDHs [38]

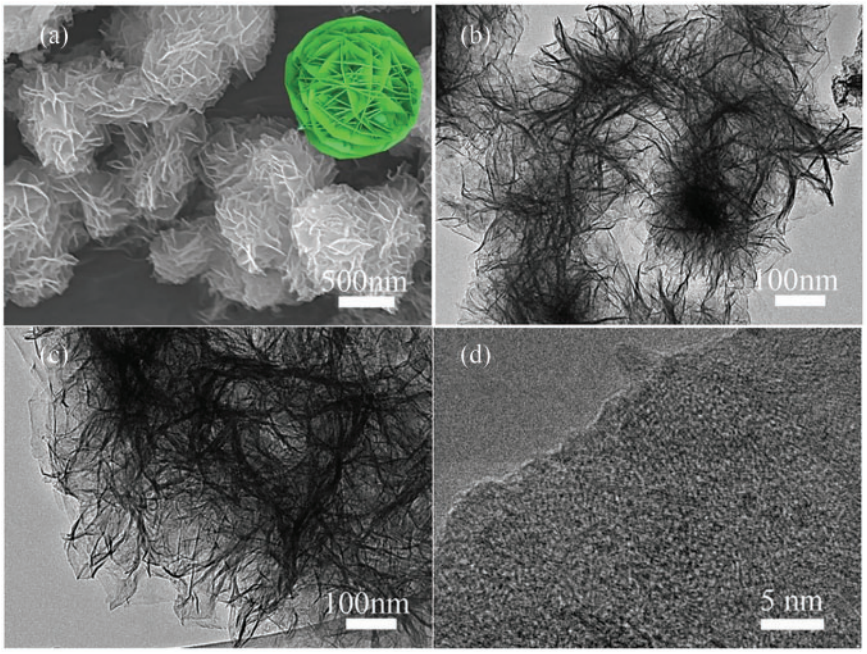

Figure 4: The FESEM and TEM image of NiCoMn-OH sample [41]

3.3 Introducing Oxygen Vacancies

Oxygen vacancies, formed by the absence of oxygen atoms in the crystal lattice of metal oxides, can lower the activation barrier for ion diffusion, increase carrier concentration, and enhance surface redox reactions. Introducing oxygen vacancy defects into LDHs can boost their reversible redox reactions and capacitive properties [4,43].

Tang et al. [44] prepared layered nickel-manganese double hydroxide (Ni-Mn-LDHs) on nickel foam via *in-situ* electrodeposition and investigated the relationship between oxygen vacancies and reversible redox reactions by adjusting the oxygen vacancy concentration and morphology of Ov-NiMn-LDH. Results indicate that oxygen vacancy regulation benefits the reaction between LDHs and OH^-. Fig. 5 illustrates the schematic diagram of the Ov-LDH 3D structure.

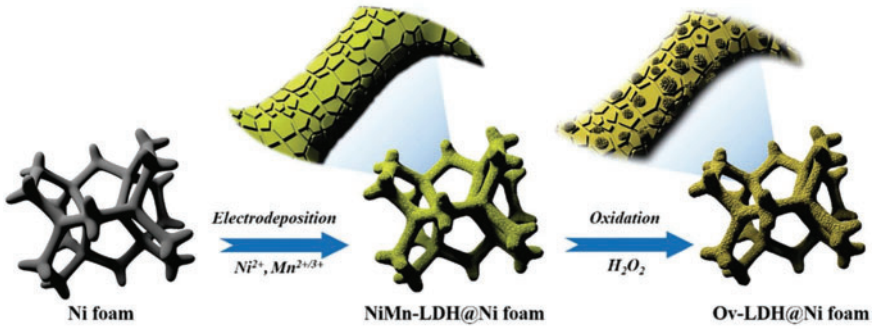

Figure 5: Schematic diagram of Ov-LDH 3D structure [44]

Wang et al. [45] treated hydrothermally synthesized CoAl-LDHs with $NaBH_4$ and assessed the electrochemical properties of Ov-CoAl-LDHs. Results showed that oxygen vacancy quantity correlates with treatment time, and an optimal amount enhances electrochemical performance. Under the best conditions, the SC value of CoAl-LDHs reaches 799.2 F/g at 1 A/g, about 1.4 times that of untreated samples, and retains 81.1% at 20 A/g. Fig. 6 displays the samples' FESEM, TEM, and element mapping.

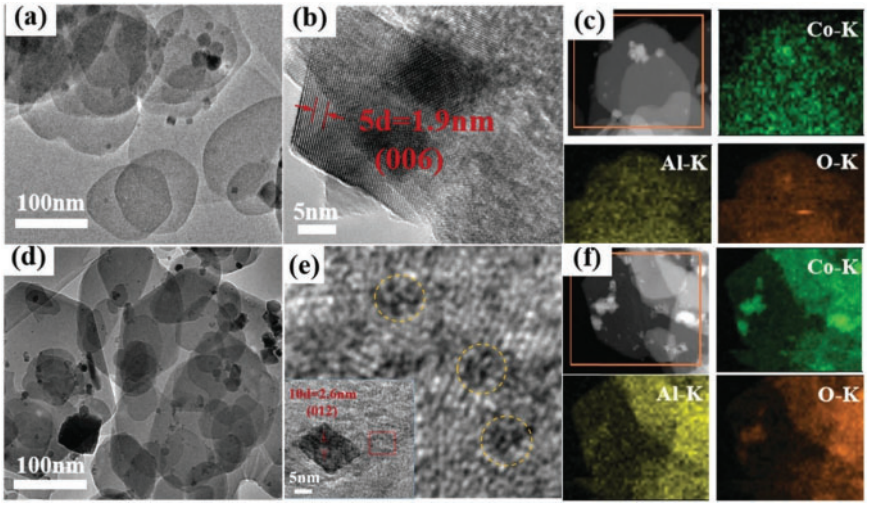

Figure 6: FESEM and TEM images of CoAl-LDHs (a and b) and CoAl-LDHs-0.5 (d and e). Elemental mappings of CoAl-LDHs (c) and CoAl-LDHs-0.5 (f) [45]

The concise test results of the main references in this chapter are shown in Table 1.

Table 1: LDH electrode and its rate capacity for enhancing intrinsic reaction activity strategy

Enhancing the intrinsic reactivity of materials					
Sample	**Current density**	**Specific capacitance**	**Current density**	**Specific capacitance**	**Ref.**
Ni-Co-Al-LDH	1 A/g	2062 F/g	10 A/g	1005 F/g	[36]
Ni-Co-LDH	0.5 A/g	1587.5 F/g	10 A/g	1155 F/g	[37]
Ni-Co-Mn-LDH	2 A/g	Greater than 2000 F/g	80 A/g	1250 F/g	[38]
Ni-Co-P-LDH	1 A/g	1340 F/g	20 A/g	749 F/g	[39]
NiCo-OH-LDH	1 A/g	888 C/g	50 A/g	662 C/g	[42]
Ov-NiMn-LDH	1 A/g	1183 C/g	10 A/g	835 C/g	[44]
Ov-CoAl-LDHs	1 A/g	799.2 F/g	20 A/g	647.4 F/g	[45]

4 Increasing Specific Surface Area

4.1 Nano-Crystallization

Nanoization of materials can increase their SSA. By leveraging the characteristics of nanomaterials, the preparation of nanoscale LDHs materials can increase their SSA, thereby enhance the material's charge storage performance.

Zhao et al. [46] synthesized Ni-Ti-LDHs nanosheets via inverse microemulsion. Their research shows that LDHs with ultra-thin nanosheet structures have higher SSA and electrolyte contact area, significantly improving energy storage. The SC values were 2310 F/g at 1.5 A/g and 1206 F/g at 30 A/g. Yang et al. [47] fabricated Ni-Co-LDHs ultra-thin nanosheets through surface restricted growth of graphene oxide. With lateral dimensions of about 1.7–1.8 nm, these nanosheets exhibited SC values of 1489 F/g at 1 A/g and 1007 F/g at 100 A/g, compared to 932 F/g and 413 F/g for bulk materials. Fig. 7 presents the microstructure of Ni-Co-LDHs ultra-thin nanosheets.

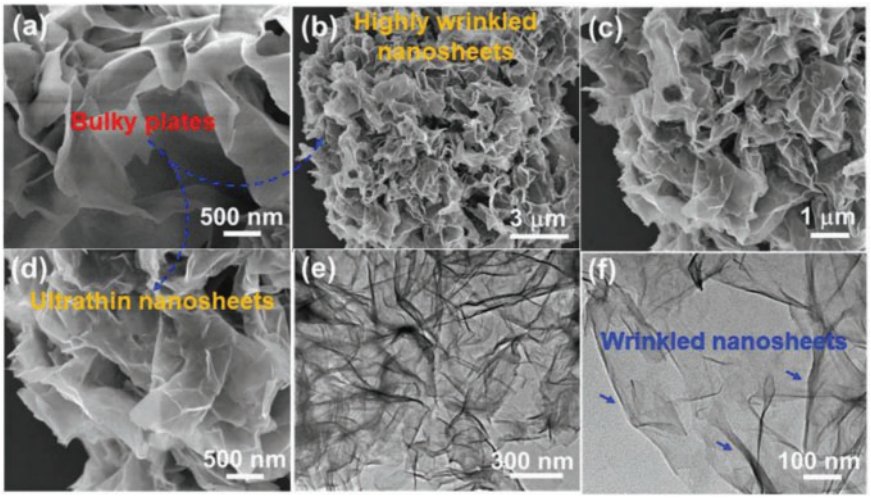

Figure 7: Microstructure of Ni-Co-LDHs ultra-thin nanosheets [47]

Liu et al. [48] used a Co-Al-LDHs nanosheet array with interlayer Co_3^{2-} as a precursor. They obtained a Co-Al_2O_3-CoO composite by controlling calcination in a hydrogen atmosphere. After recovering Co-Al_2O_3-CoO in a Co_3^{2-} containing solution, they regenerated a nano hierarchical CoAl-LDHs nanosheet array with interlayer Co_3^{2-}. Tests showed the treated array had SC values of 883 F/g at 1 A/g and 468 F/g at 40 A/g, surpassing the untreated values of 588 and 188 F/g.

4.2 Building Hierarchical Structures

Material aggregation during synthesis reduces SSA and active sites. To enhance LDHs electrode performance, reducing agglomeration improves SSA and charge storage. Hierarchical current collector structures increase their SSA, boost LDHs loading, and mitigate synthesis related agglomeration. Using this approach, researchers have synthesized various LDHs on 1D, 2D, and 3D nano supports, achieving good results [49–52].

Yu et al. [53] synthesized Co-Al-LDHs nanosheets by adding carbon nanotubes (CNTs) directly in hydrothermal. CNTs are embedded between nanosheets as support and conductive material. Electrochemical tests show an SC of 884 F/g at 5 mA/cm², retaining 88% after 2000 cycles at 10 mA/cm². Co-Al-LDHs

nanosheets with CNTs exhibit excellent electrochemical performance. Zhang et al. [54] first *in-situ* grew ZIF-67 on polypyrrole nanotubes, then synthesized nanocage-like nickel cobalt hydroxide via hydrothermal method using ZIF-67 as precursor and divalent cobalt ion source. Yang et al. [55] first reduced GO on nickel foam, then electrodeposited flower-shaped Ni-Co-LDHs nanosheets on rGO/NF. The large area nanosheet array enhances the SSA of Ni-Co@rGO-NF, leading to excellent electrochemical performance. Tests show the electrode's SC reaches 5.820 C/cm² at 20 mA/cm², with 78% capacity retention after 2000 cycles at 100 mA/cm². Fig. 8 presents the morphology of Ni-Co DHNS@rGO-NF samples.

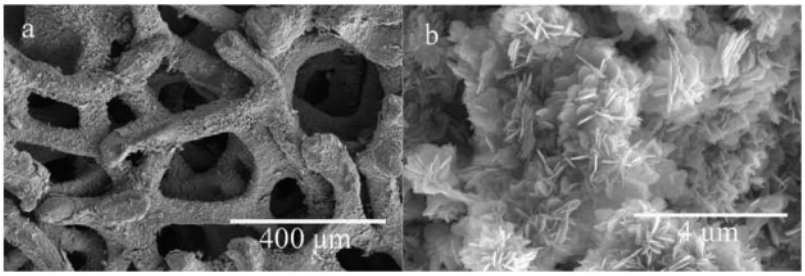

Figure 8: Morphology of Ni-Co DHNS@rGO-NF [54]

The core-shell structure can mitigate material agglomeration during synthesis, promoting full electrolyte contact [56,57]. It is a strategy to boost material SSA in material research. Zhao et al. [58] prepared $MnCo_2O_4$@$Ni(OH)_2$ core-shell nanoflowers using hexamethylenetetramine as a shape-directing agent. This structure leverages the properties of $MnCo_2O_4$ and $Ni(OH)_2$, enhancing structural stability and charge storage. The SC value reaches 2154 F/g at 5 A/g, quadrupling that of the $MnCo_2O_4$ electrode. Fig. 9 illustrates the electrode design process. Yan et al. [59] first synthesized a $NiCo_2O_4$ film on nickel foam via hydrothermal synthesis, then deposited MnO_2 on it potentiostatically to obtain MnO_2@$NiCo_2O_4$. This core-shell material, featuring $NiCo_2O_4$ nanowires as the core and MnO_2 nanosheets as the shell, has a unique 3D porous structure. Tests show an SC value of 1186 F/g at 1 A/g. Shao et al. [60] synthesized NiAl-LDHs shells on SiO_2 microspheres, creating hollow, yolk-shell, and core-shell structures by etching SiO_2. Tests indicate graded structures have larger SSA and better rate capability, with the hollow structure reaching 127 m²/g. Fig. 10 shows TEM and SEM images of these samples.

Figure 9: Schematic illustration of the general electrode design process [58]

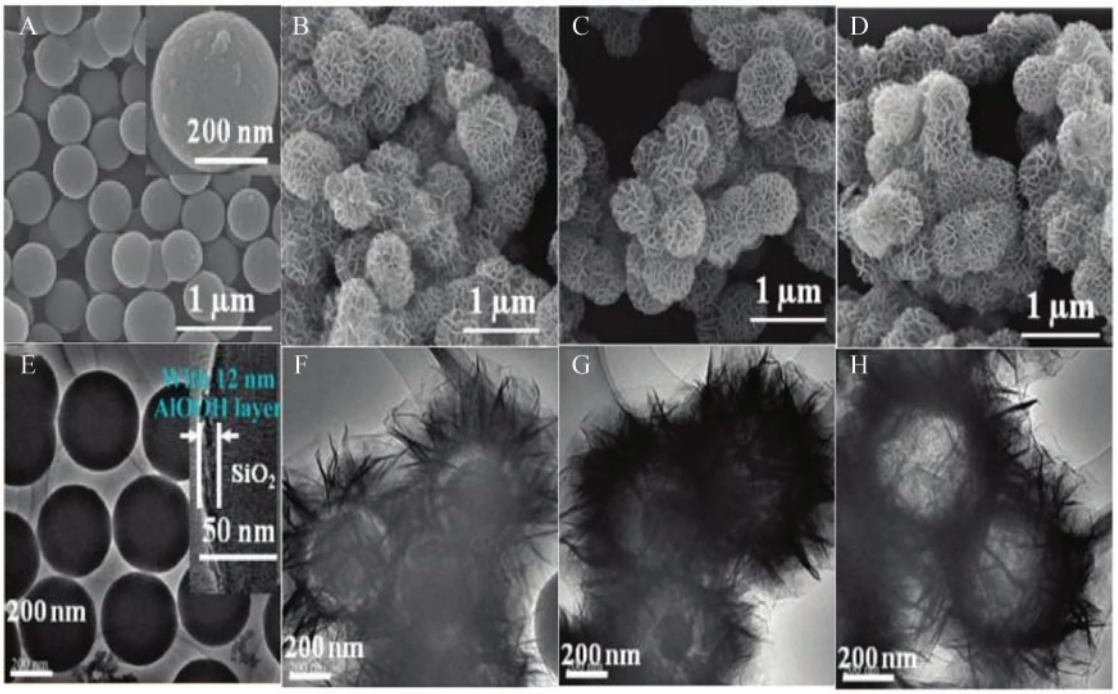

Figure 10: TEM and SEM images of samples with different structures [60]

The concise test results of the main references in this chapter are shown in Table 2.

Table 2: LDH electrode and its rate capacity for improving material specific surface area strategy

Increasing specific surface area					
Sample	**Current density**	**Specific capacitance**	**Current density**	**Specific capacitance**	**Ref.**
Ni-Ti-LDH	1.5 A/g	2310 F/g	30 A/g	1206 F/g	[46]
Ni-Co-LDH	1 A/g	1489 F/g	100 A/g	1007 F/g	[47]
Co-Al-LDH-CNTs	5 mA/cm^2	884 F/g	25 mA/cm^2	529 F/g	[53]
Ni-Co-DHNS@rGO-NF-LDH	20 mA/cm^2	5.820 C/cm^2	100 mA/cm^2	4.24 C/cm^2	[55]
$MnCo_2O_4$@Ni$(OH)_2$-LDH	5 A/g	2154 F/g	20 A/g	702 F/g	[58]
MnO_2@$NiCo_2O$-LDH	1 A/g	1186 F/g	10 A/g	596 F/g	[59]
SiO_2/Ni-Al-LDH	2 A/g	406 F/g (core-shell, 42.3 m^2/g) 524 F/g (yolk-shell, 68.5 m^2/g) 735 F/g (hollow, 124.7 m^2/g)	25 A/g	195 F/g (core-shell, 42.3 m^2/g) 343 F/g (yolk-shell, 68.5 m^2/g) 548 F/g (hollow, 124.7 m^2/g)	[60]

5 Improving Electronic Transmission

5.1 Composite with Conductors

As semiconductor materials, LDHs have poor conductivity, which limits their energy storage. A viable solution is to composite them with highly conductive, large SSA materials [61]. Common conductive materials with high SSA include nano-carbon materials, conductive polymers, phosphides, sulfides, etc. [62–64].

Yang et al. [65] prepared flower-shaped $Ni(OH)_2$ microspheres in their high-performance supercapacitor study. Using a two-step synthesis strategy based on Ni/PC, the SC value of the prepared Ni/PC reached 1960 F/g at 1 A/g, showing excellent cycling stability. Tang et al. [34] used hydrothermal synthesis to composite CNT with $Ni_{0.3}$CoAl-LDH, improving conductivity. The prepared CNT/$Ni_{0.3}$CoAl-LDH had a specific capacity of 1332 F/g at 1 A/g, nearly 30% higher than the control group. At 10 A/g, the specific capacity retention was 60.4%, 40% higher than the control group, with an 87.6% capacity retention rate after 3000 cycles at 5 A/g. Mohamed et al. [66] prepared graphene/Zn-Al-LDHs composite materials by combining Zn-Al-LDHs with graphene. Tests showed the electrode achieved the highest SC value of 140 F/g at a scan rate of 10 mV/s. After 2000 charge-discharge cycles, the initial capacitance remained at 97%. Fig. 11 shows the morphology of Zn-Al-LDHs and graphene nanosheets.

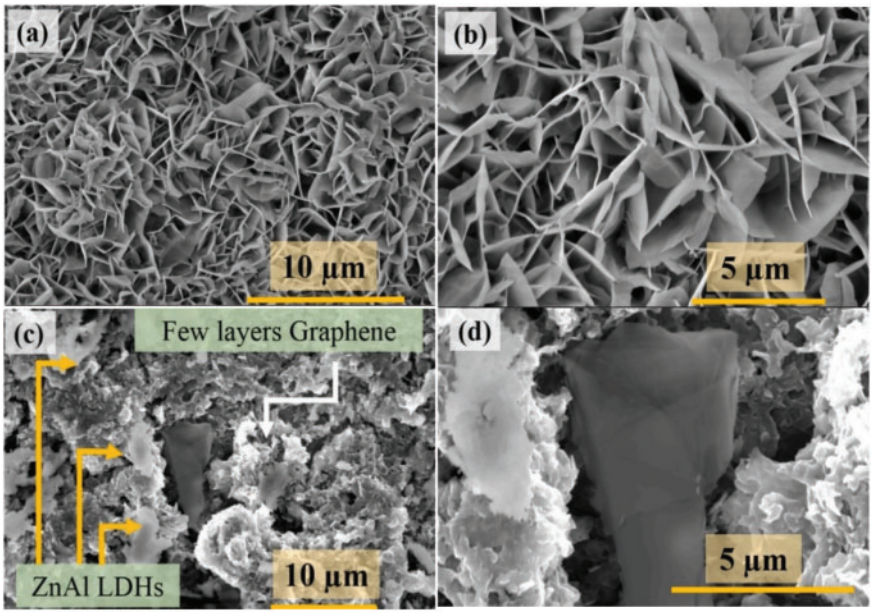

Figure 11: Morphology of Zn-Al-LDHs and graphene nanosheets [66]

Conductive polypyrrole (PPy) is an ideal conductive additive for expanding the surface area of nanosheets. Liang et al. [67] fabricated a rGO/PPy/Ni-Co-LDH hybrid composite with a sandwich structure in a simple way. Polypyrrole is doped into nanosheets as a conductive material and can also serve as an intermediate layer to expand the surface area. The SC value of rGO/PPy/Ni-Co-LDH reached 2534 F/g at 1 A/g, and after 5000 cycles, it still reached 1976.5 F/g. Fig. 12 shows the synthesis steps of rGO/PPy/Ni-Co-LDH composite material.

MXenes, with good conductivity, excellent specific capacity, and chemical stability, can enhance electron transport and rate capacity when combined with LDHs. Wang et al. [68] incorporated Ti_3C_2 nanosheets into

a Ni and Al salt solution and used solvothermal method to prepare NiAl-LDHs/Ti_3C_2 composites. These composites have SC values of 1061 F/g at 1 A/g and 556 F/g at 10 A/g. Fig. 13 shows the morphologies of MXene and MXene/LDHs composite. Zhang et al. [69] used nickel nitrate, manganese sulfate, and exfoliated Ti_3C_2 as raw materials to prepare NiMn-LDHs/Ti_3C_2 composites via chemical precipitation. These composites exhibit SC values of 1575 F/g at 0.5 A/g and 1253 F/g at 20 A/g, surpassing pure NiMn-LDHs' 689 F/g at 0.5 A/g and 69 F/g at 20 A/g.

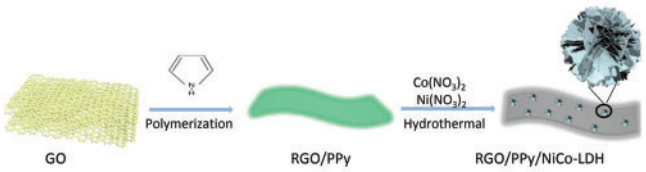

Figure 12: Synthesis steps of rGO/PPy/Ni-Co-LDH composite material [67]

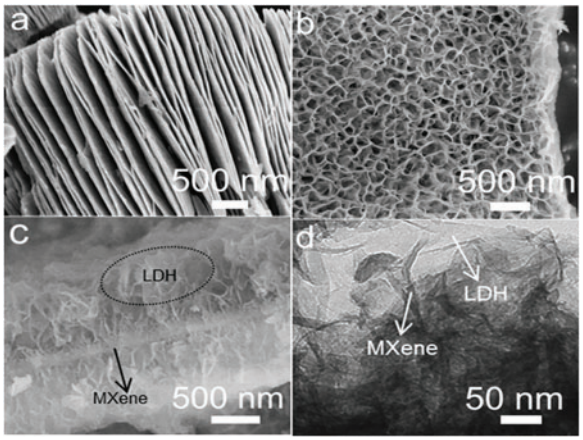

Figure 13: Morphologies of the MXene and MXene/LDHs composite material [68]

5.2 Deposition Growth on Conductive Substrates

Using copper, aluminum, nickel, or stainless steel as substrates, directly depositing/growing LDHs on the substrate avoids conductive and adhesive agents during electrode preparation, yielding an integrated electrode. This method prevents charge transfer interference from adhesives between LDHs and substrate, enhancing charge transfer efficiency.

Li et al. [70] fabricated Ni-Co-LDHs electrodes on carbon fiber cloth via electrodeposition without adhesives or conductive agents, obtaining an ultra-thin nanostructured electrode. The SC value reaches 1540 F/g at 1 A/g, with 82.9% retention after 5000 cycles at 10 A/g, indicating good cycling stability. Wu et al. [71] used oxalic acid to *in-situ* grow $NiCo_2O_4$ on nickel foam. The $NiCo_2O_4$/foam nickel composite electrode benefits from the substrate's 3D network and conductivity, showing excellent electron and ion transport, rate capability, and cycle stability. It has an SC of 514.22 F/g at 1 A/g, 432.4 F/g at 10 A/g, and 92% capacitance retention after 2000 cycles at 2 A/g. Qi et al. [72] *in-situ* generated Zn-Ni double hydroxides nanosheets on nickel foam via chemical deposition. SEM images show uniform attachment, forming a porous nanosheet array. Electrochemical tests revealed an SC of 746.2 F/g at 1 A/g, retaining 70.9% after 3000 cycles. Li et al. [73] developed a high SSA porous oxide thin film on 304 stainless-steel via constant pressure

anodizing. This stainless-steel based film, acting as a high-performance active electrode, needs no binders or current collectors. It shows an SC of 125.6 mF/cm² at 1 mA/cm², retaining over 75% after 1000 cycles, indicating good electrochemical performance.

5.3 Improving Ion Transport

Layer spacing in LDHs is crucial for their capacitance. Wider spacing benefits the swift and reversible insertion/removal of electrolyte ions and boosts active sites for electrochemical reactions, improving theoretical capacitance utilization [35,60]. Introducing columnar anions or macromolecules can increase layer spacing. Thus, enlarging layer spacing by interlayer ion regulation is key to enhancing LDHs' capacitance performance.

Wang et al. [74] used sodium dodecyl sulfonate (SDS) as intercalating agent and soft template to load Ni-Mn-LDHs on foam nickel by one-step hydrothermal method, achieving high load capacity and high capacitance performance. The electrode with 4 mmol SDS added achieved a maximum load of 4.9 mg/cm^2, a maximum area capacitance of 6311 mF/cm^2, and the highest rate performance (52%) at a current density of 5 mA/cm^2. Xiao et al. [75] prepared Co-Al-LDHs with interlayer spacing of 0.76, 0.87, and 2.58 nm using CO_3^{2-}, SO_4^{2-}, and dodecyl sulfate as intercalation anions using a hydrothermal method. Related tests have shown that Co-Al-LDHs samples with a 2.58 nm interlayer spacing have the best charge transfer performance. The SC values of the samples at 1 and 32 A/g reached 1481.7 and 856.7 F/g, respectively. Lin et al. [76] synthesized Ni-Co-LDHs with large interlayer spacing using dodecyl benzenesulfonic acid as the intercalation anion. The experiment used hydrothermal method as the preparation method, and the interlayer spacing of Ni-Co-LDHs prepared reached 1.53 nm. The SC value at 3 A/g reached 1646 F/g. Fig. 14 shows the microstructure of CoAl-LDHs with different intercalation ions.

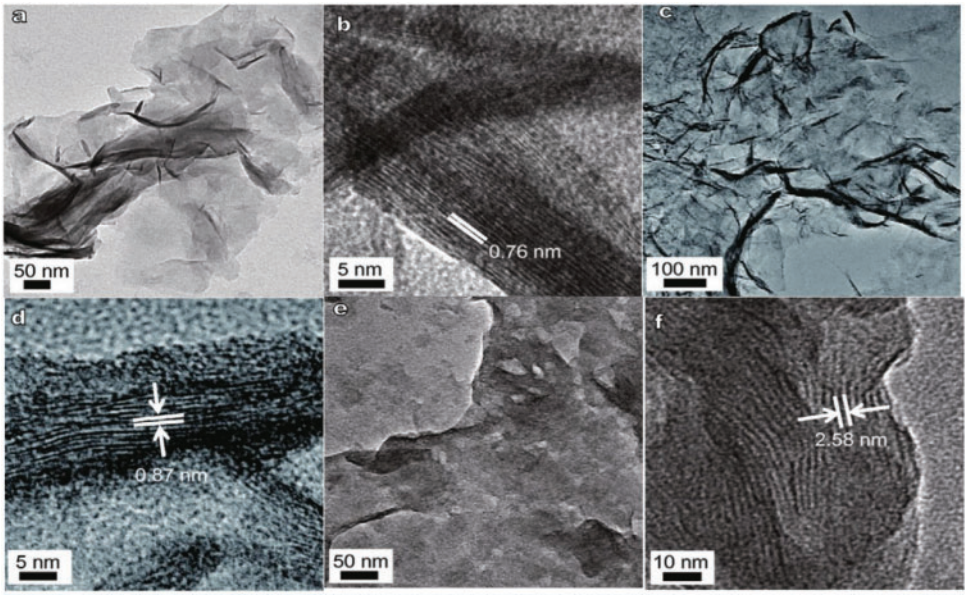

Figure 14: Microstructure of CoAl-LDHs with different intercalation ions (a–b) CO_3^{2-}, (c–d) SO_4^{2-} and (e–f) DS– samples [75]

Wang et al. [74] used sodium dodecyl sulfonate (SDS) as an intercalating agent and soft template to load Ni-Mn-LDHs on nickel foam via one-step hydrothermal synthesis, achieving high loading and

capacitance. The electrode with 4 mmol SDS reached a maximum loading of 4.9 mg/cm², a maximum area capacitance of 6311 mF/cm², and the highest rate performance (52%) at 5 mA/cm². Xiao et al. [75] prepared Co-Al-LDHs with interlayer spacings of 0.76, 0.87, and 2.58 nm using CO_3^{2-}, SO_4^{2-}, and dodecyl sulfate as intercalation anions via hydrothermal synthesis. The 2.58 nm spaced Co-Al-LDHs showed the best charge transfer performance, with SC values of 1481.7 F/g at 1 A/g and 856.7 F/g at 32 A/g. Lin et al. [76] synthesized Ni-Co-LDHs with large interlayer spacing using dodecyl benzenesulfonic acid as the intercalation anion via hydrothermal method. The interlayer spacing reached 1.53 nm, and the SC value at 3 A/g reached 1646 F/g. Fig. 14 shows the microstructure of CoAl-LDHs with different intercalation ions.

Macromolecule intercalation enhances the capacitance of LDHs. Glucose and ethylene glycol, with negatively charged OH^- groups, intercalate via electrostatic interaction with LDHs' positively charged layers. This not only expands the interlayer spacing but also optimizes the phase structure, improving stability. Quan et al. [77] *in-situ* grew Ni-Mn hydroxide nanowire arrays on nickel foam and used glucose to intercalate and coat a Co_3O_4 layer. Tests showed glucose insertion increased the crystal plane spacing of Ni-Mn hydroxide nanosheets from 7.49 to 8.27 Å. Supercapacitors using this material as the working electrode achieved an SC value of 1644 F/g at 1 A/g and showed excellent cycling stability. Fig. 15 illustrates the preparation of Co_3O_4@NiMn-LDH-m/NF heterostructures.

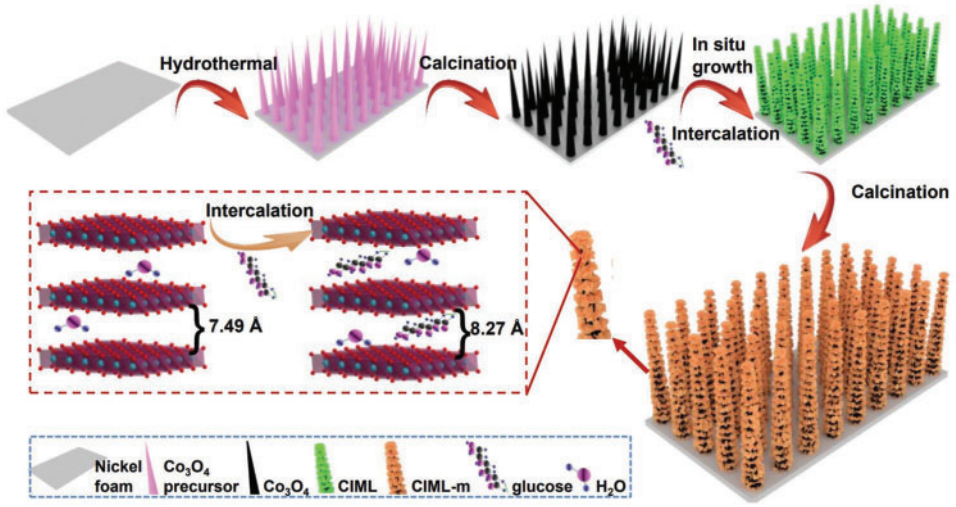

Figure 15: The preparation process of Co_3O_4@NiMn-LDH-m/NF heterostructures [77]

The concise test results of the main references in this chapter are shown in Table 3.

Table 3: LDH electrode and its rate capacity for improving electronic transmission strategy

Improving electronic transmission					
Sample	**Current density**	**Specific capacitance**	**Current density**	**Specific capacitance**	**Ref.**
Ni/PC-LDH	1 A/g	1960 F/g	10 A/g	760 F/g	[65]
rGO/PPy/Ni-Co-LDH	1 A/g	2534 F/g	10 A/g	1837 F/g	[67]

(Continued)

Table 3 (continued)

Improving electronic transmission					
Sample	**Current density**	**Specific capacitance**	**Current density**	**Specific capacitance**	**Ref.**
Ni-Al/ Ti_3C_2-LDH	1 A/g	1061 F/g	10 A/g	556 F/g	[68]
NiMn/Ti_3C_2-LDH	0.5 A/g	1575 F/g	20 A/g	1260 F/g	[69]
Ni-Co-LDH/CFC	1 A/g	1540 F/g	15 A/g	1284.5 F/g	[70]
$NiCo_2O_4$-LDH/NF	1 A/g	514.22 F/g	10 A/g	432.4 F/g	[71]
Ni@Zn-Ni LDHs	1 A/g	746.2 F/g	10 A/g	610 F/g	[72]
Co-Al-LDH	1 A/g (The interlayer distance is 2.58 nm)	1481.7 F/g	1 A/g (The interlayer distance is 0.76 nm)	1149.2 F/g	[75]
Ni-Co/SDBS-LDH	3 A/g	1646 F/g	10 A/g	680 F/g	[76]
3D core-shell Co_3O_4@NiMn-LDH	1 A/g (The interlayer distance is 8.27 nm)	1644 F/g	10 A/g (The interlayer distance is 8.27 nm)	697 F/g	[77]

6 Summary and Outlook

This article outlines LDHs' basic structure and electrochemical mechanisms. It also summaries key methods to enhance their rate capacity, which can be grouped into three categories: boosting reaction activity, expanding active SSA, and improving charge transfer kinetics. For reaction activity enhancement, component regulation, amorphization, and oxygen vacancy introduction are the main approaches. To increase active SSA, nanosizing and hierarchical structure construction can raise LDHs' surface area and active site exposure. For charge transfer dynamics, combining with good conductors, *in-situ* growth of conductive substrates, and layer spacing expansion are the primary strategies. These research methods effectively improve LDHs' rate capacity. However, developing high-rate capacity LDH electrode materials for practical supercapacitor applications remains challenging. Future research should focus on the following aspects based on current research.

(1) Though LDHs theoretically have high specific capacitance, their practical performance is limited by charge transfer efficiency and ion diffusion rate. Future research will focus on designing nanostructures like nanosheets and nanowires to shorten ion diffusion distance and enhance rate performance. At the same time, defect engineering will be used to introduce lattice defects, increasing active sites and specific capacitance. For example, creating oxygen vacancies on LDH nanosheets via chemical etching can boost ion adsorption and storage, achieving higher specific capacitance at high current densities.

(2) When designing LDH electrodes, the synergistic effect between material reactivity and charge transfer should be considered to avoid the "barrel effect". After obtaining a high SSA hierarchical structure, new composite strategies should be developed, such as combining LDHs with conductive carbon materials (like graphene and carbon nanotubes) or other high electron mobility materials. This improves overall electron transfer and achieves the coordinated enhancement of high specific capacitance and high-rate performance.

(3) Currently, LDHs face issues like structural degradation and active substance loss during cycling. Future solutions will focus on material and interfacial stability. For structural stability, interlayer supports or multi-layer composites can be introduced to enhance interlayer interaction and prevent layer collapse during charge-discharge. For example, organic molecules or inorganic nanoparticles can stabilize the LDH layered structure and extend cycle life.

(4) Existing synthesis methods have limitations in controlling the crystal structure, particle size distribution, and compositional uniformity of LDHs. In the future, high-precision techniques like atomic layer deposition (ALD) and molecular beam epitaxy (MBE) will be more widely applied. These technologies enable atomic-scale control of LDH growth, allowing the preparation of materials with highly ordered structures and precise composition ratios, thus achieving precise property regulation. For example, ALD can be used to grow LDH nanofilms layer by layer, precisely controlling film thickness and composition, providing a basis for high-performance micro energy storage device preparation.

Acknowledgement: Not applicable.

Funding Statement: This work was supported by Suzhou University Doctoral Initiation Fund and Open Project (2020BS009, 2013YKF24), Anhui Provincial Department of Education Natural Science Foundation (2022AH051386, 2023KYTD01), Anhui Higher Education Quality Engineering Project (2022jyxm1595, 2020gnxm070), Teaching Research Project of Suzhou University (szxy2024jyjf55, 2021jyxm1502).

Author Contributions: Conceptualization, Jie Yang; methodology, Jie Yang; software, Hengzheng Li; validation, Jie Yang and Hengzheng Li; formal analysis, Hengzheng Li; investigation, Hengzheng Li; resources, Hengzheng Li; data curation, Hengzheng Li; writing—original draft preparation, Hengzheng Li; writing—review and editing, Jie Yang and Hengzheng Li; visualization, Hengzheng Li; supervision, Jie Yang; project administration, Jie Yang; funding acquisition, Hengzheng Li. All authors reviewed the results and approved the final version of the manuscript.

Availability of Data and Materials: Not applicable.

Ethics Approval: Not applicable.

Conflicts of Interest: The authors declare no conflicts of interest to report regarding the present study.

References

1. Theerthagiri J, Karuppasamy K, Raj CJ, Maia G, Kumari ML, Kennedy JL, et al. Structural engineering of metal oxyhydroxide for electrochemical energy conversion and storage. Coord Chem Rev. 2024;513:215880. doi:10.1016/j.ccr.2024.215880.
2. Panda S, Deshmukh K, Khadheer PSK, Theerthagiri J, Manickam S, Choi MY. MXene based emerging materials for supercapacitor applications: recent advances, challenges, and future perspectives. Coord Chem Rev. 2022;462:214518. doi:10.1016/j.ccr.2022.214518.
3. Yao L, Geng ZB, Zhang W, Wu XF, Liu JH, Li LP, et al. *In situ* growth of amorphous nife hydroxides on spinel $NiFe_2O_4$ via ultrasonic-assisted reduction for an enhanced oxygen evolution reaction. ACS Sustain Chem Eng. 2021;8:17194–200. doi:10.1021/acssuschemeng.0c05888.
4. Yan D, Wang W, Luo X, Chen C, Zeng Y, Zhu ZH. $NiCo_2O_4$ with oxygen vacancies as better performance electrode material for supercapacitor. Chem Eng J. 2018;334:864–72. doi:10.1016/j.cej.2017.10.128.

5. Xie LJ, Hu ZG, Lv CH, Sun GH, Wang JL, Li YQ. Co_xNi_{1-x} double hydroxide nanoparticles with ultrahigh specific capacitances as supercapacitor electrode materials. Electrochim Acta. 2012;78:205–11. doi:10.1016/j.electacta.2012.05.145.
6. Li HB, Gao YQ, Wang CX, Yang GW. A simple electrochemical route to access amorphous mixed-metal hydroxides for supercapacitor electrode materials. Adv Energy Mater. 2015;5(6):1–9.
7. Nasser R, Jian TT, Song JM. Hierarchical porous activated carbon derived from olives: preparation, (N, S) co-doping, and its application in supercapacitors. J Energy Storage. 2022;51:104348. doi:10.1016/j.est.2022.104348.
8. Pelin O, Ceren D, Hakan D, Ugur M, Salim E, Canan S, et al. Activated carbons prepared from hazelnut shell waste by phosphoric acid activation for supercapacitor electrode applications and comprehensive electrochemical analysis. Renew Energy. 2022;189:535–48. doi:10.1016/j.renene.2022.02.126.
9. Aleem A, Rashmi AB, Dipak GB, Shivram SG. One pot solvothermal synthesis of bimetallic copper iron sulfide ($CuFeS_2$) and its use as electrode material in supercapacitor applications. Appl Surf Sci Adv. 2022;9:100231. doi:10.1016/j.apsadv.2022.100231.
10. Jiao C, Zhang WK, Su FY, Yang HY, Liu RX, Chen CM. Research progress on electrode materials and electrolytes for supercapacitors. New Carbon Mater. 2017;32:106–15.
11. Murali G, Kesavan T, Anandha BG, Ponnusamy S, Harish S, Navaneethan M. Improved supercapacitor performance based on sustainable synthesis using chemically activated porous carbon. J Alloys Comp. 2022;906:164287. doi:10.1016/j.jallcom.2022.164287.
12. Raissa V, Rafael V, Lenon HC, Reinaldo T, Leonardo MDS, Hudson Z. *In-situ* electrochemical and operando Raman techniques to investigate the effect of porosity in different carbon electrodes in organic electrolyte supercapacitors. J Energy Storage. 2022;50:104219. doi:10.1016/j.est.2022.104219.
13. Aziz MA, Shah SS, Nayem SM, Shaikh MN, Hakeem AS, Bakare IA. Peat soil-derived silica doped porous graphitic carbon with high yield for high-performance all-solid-state symmetric supercapacitors. J Energy Storage. 2022;50:104278. doi:10.1016/j.est.2022.104278.
14. Belaineh D, Brooke R, Sani N, Say MG, Håkansson KMO, Engquist I, et al. Printable carbon-based supercapacitors reinforced with cellulose and conductive polymers. J Energy Storage. 2022;50:104224. doi:10.1016/j.est.2022.104224.
15. Murni H, Yhana M, Anggoro MA, Aumber A, Iwan S, Farid T, et al. One-pot synthesis of reduced graphene oxide/chitosan/zinc oxide ternary nanocomposites for supercapacitor electrodes with enhanced electrochemical properties. Mater Lett. 2022;314:131846. doi:10.1016/j.matlet.2022.131846.
16. Attia SY, Mohamed SG. Detergent-free micelle-assisted synthesis of carbon-containing hexagonal CuS nanostructures for efficient supercapacitor electrode materials. Electrochim Acta. 2022;407:139918. doi:10.1016/j.electacta.2022.139918.
17. Xia JL, Chen F, Li JH, Tao NJ. Measurement of the quantum capacitance of graphene. Nat Nanotechnol. 2009;4:505–9. doi:10.1038/nnano.2009.177.
18. Alqarni AN, Cevik E, Gondal MA, Almessiere MA, Baykal A, Bozkurt A, et al. Synthesis and design of vanadium intercalated spinal ferrite ($Co_{0.5}Ni_{0.5}VxFe_{1.6-x}O_4$) electrodes for high current supercapacitor applications. J Energy Stor. 2022;51:104357. doi:10.1016/j.est.2022.104357.
19. Liu ZQ, Zhong YX, Qiu YL. Multilayered and hierarchical structured NiCo double hydroxide nanosheets generated on porous $MgCo_2O_4$ nanowire arrays for high performance supercapacitors. Appl Surf Sci. 2021;546:149133. doi:10.1016/j.apsusc.2021.149133.
20. Ding YJ. Preparation and modification of nickel cobalt layered double hydroxides and their performances for supercapacitors. Wuhan, China: Jianghan University; 2024.
21. Li ZH, Duan Ha H, Shao MF, Li JB, O, Hare D, Wei M, et al. Ordered-vacancy-induced cation intercalation into layered double hydroxides: a general approach for high-performance supercapacitors. Chem. 2018;4(9):2168–79. doi:10.1016/j.chempr.2018.06.007.
22. An Z, He J, Duan X. Catalysts with catalytic sites highly dispersed from layered double hydroxide as precursors. Chin J Catal. 2013;34(1):225–34. doi:10.3724/SP.J.1088.2013.20870.

23. Ali M, Pouria K, Saeedeh M, Mohammad BA, Farhad S. Bimetallic nickel-cobalt oxide nanoparticle/electrospun carbon nanofiber composites: preparation and application for supercapacitor electrode. Ceramics Int. 2022;48(7):10015–23. doi:10.1016/j.ceramint.2021.12.210.
24. Quan W, Tang ZL, Hong Y, Wang ST, Zhang ZT. Hydroxyl compensation effects on the cycle stability of nickel-cobalt layered double hydroxides synthesized via solvothermal method. Electrochim Acta. 2015;182:445–51. doi:10.1016/j.electacta.2015.09.118.
25. Siva V, Murugan A, Shameem A, Thangarasu S, Bahadur SA. A facile microwave-assisted combustion synthesis of $NiCoFe_2O_4$ anchored polymer nanocomposites as an efficient electrode material for asymmetric supercapacitor application. J Energy Storage. 2022;48:103965. doi:10.1016/j.est.2022.103965.
26. Heo JY, Rajangam V, Kim H, Babu RS, Kumar KK, Gopi CVV, et al. Template and binder free 1D cobalt nickel hydrogen phosphate electrode materials for supercapacitor application. J Ind Eng Chem. 2022;106:328–39. doi:10.1016/j.jiec.2021.11.010.
27. Maryam A, Saied DHS, Seyyed ME, Fu YQ. Cobalt-molybdenum selenide double-shelled hollow nanocages derived from metal-organic frameworks as high performance electrodes for hybrid supercapacitor. J Colloid Interface Sci. 2022;616:141–51. doi:10.1016/j.jcis.2022.02.063.
28. Rasmita B, Gayatree B, Vaishali T, Pravin PI. Supercapacitor performance and charge storage mechanism of brannerite type CuV_2O_6/PANI nanocomposites synthesis with their theoretical aspects. Electrochim Acta. 2022;410:140015. doi:10.1016/j.electacta.2022.140015.
29. Nandhini S, Muralidharan G. The binder-free mesoporous $CoNi_2S_4$ electrode for high-performance symmetric and asymmetric supercapacitor devices. J Mater Sci. 2022;57:5933–53. doi:10.1007/s10853-022-06987-2.
30. Zingare PA, Dhoble SJ, Deshmukh AD. Highly stable fish-scale derived lamellar carbon for high performance supercapacitor application. Diam Relat Mater. 2022;124:108925. doi:10.1016/j.diamond.2022.108925.
31. Akbar MZ, Bahareh A, Saied SHD. Fabrication of hollow $MnFe_2O_4$ nanocubes assembled by CoS_2 nanosheets for hybrid supercapacitors. Chem Eng J. 2022;435(P3):135170. doi:10.1016/j.cej.2022.135170.
32. Seungju J, Nagabandi J, Daewon K. Rational design of cobalt-iron bimetal layered hydroxide on conductive fabric as a flexible battery-type electrode for enhancing the performance of hybrid supercapacitor. J Alloys Comp. 2022;904:164082. doi:10.1016/j.jallcom.2022.164082.
33. Li H, Lin S, Li H, Wu ZQ, Chen Q, Zhu LL, et al. Magneto-electrodeposition of 3D cross-linked NiCo-LDH for flexible high-performance supercapacitors. Small Methods. 2022;06:2101320. doi:10.1002/smtd.202101320.
34. Tang AJ, Mi CH, Chen PP. Preparation of NiCoAl-LDH with different Ni contents and electrochemical performance of CNT/$Ni_{0.3}$CoAl LDH material. Chin J Inorg Chem. 2020;36:1906–16.
35. Xu J, Gai SL, He F, Niu N, Gao P, Chen YJ, et al. A sandwich-type three-dimensional layered double hydroxide nanosheet array/graphene composite: fabrication and high supercapacitor performance. J Mater Chem A. 2014;2(4):1022–31. doi:10.1039/C3TA14048B.
36. Wang X, Lin Y, Su Y. Design and synthesis of ternary-component layered double hydroxides for high-performance supercapacitors: understanding the role of trivalent metal ions. Electrochim Acta. 2017;225:263–71. doi:10.1016/j.electacta.2016.12.160.
37. Wei M, Huang QS, Zhou YP. Ultrathin nanosheets of cobalt-nickel hydroxides hetero-structure via electrodeposition and precursor adjustment with excellent performance for supercapacitor. J Energy Chem. 2018;27:591–9. doi:10.1016/j.jechem.2017.10.022.
38. Xiong G, He P, Liu L, Chen T, Fisher TS. Plasma-grown graphene petals templating NiCoMn hydroxide nanoneedles for high-rate and long-cycle-life pseudocapacitive electrodes. J Mater Chem A. 2015;3(45):22940–8. doi:10.1039/C5TA05441A.
39. Wang GR, Li YB, Zhao ZL, Jin ZL. Phosphatized mild-prepared-NiCo LDHs cabbage-like sphere exhibits excellent performance as supercapacitor electrode. New J Chem. 2021;45(1):251–61. doi:10.1039/D0NJ03070H.
40. Kang JX, Yang XY, Hu Q, Cai Z, Liu LM, Guo L. Recent progress of amorphous nanomaterials. Chem Rev. 2023;123(13):8859–941. doi:10.1021/acs.chemrev.3c00229.
41. Chen HC, Qin Y, Cao H. Synthesis of amorphous nickel cobalt-manganese hydroxides for supercapacitor-battery hybrid energy storage system. Energy Storage Mater. 2019;17:194–203. doi:10.1016/j.ensm.2018.07.018.

42. Huang CH, Hu YZ, Jiang SP, Chen HC. Amorphous nickel-based hydroxides with different cation substitutions for advanced hybrid supercapacitors. Electrochimica Acta. 2019;325:134936. doi:10.1016/j.electacta.2019.134936.
43. Zhang XY, Liu XQ, Zeng YX, Tong YX, Lu XH. Oxygen defects in promoting the electrochemical performance of metal oxides for supercapacitors: recent advances and challenges. Small Methods. 2020;4(6):1900823. doi:10.1002/smtd.201900823.
44. Tang YQ, Shen HM, Cheng JQ, Liang ZB, Qu C, Hassina T, et al. Fabrication of oxygen-vacancy abundant nimn-layered double hydroxides for ultrahigh capacity supercapacitors. Adv Funct Mat. 2020;30:1908223. doi:10.1002/adfm.201908223.
45. Wang GR, Jin ZL. Oxygen-vacancy-rich cobalt-aluminum hydrotalcite structure for supercapacitor cathode with high performance. J Mater Chem C. 2021;9:620–32. doi:10.1039/D0TC03640D.
46. Zhao YF, Wang Q, Bian T, Fan H, Zhou C, Wu LZ, et al. Ni^{3+} doped monolayer layered double hydroxide nanosheets as efficient electrodes for supercapacitors. Nanoscale. 2015;7:7168–73. doi:10.1039/C5NR01320H.
47. Yang J, Yu C, Hu C, Wang M, Li SF, Huang HW, et al. Surface-confined fabrication of ultrathin nickel cobalt-layered double hydroxide nanosheets for high-performance supercapacitors. Adv Funct Mater. 2018;28(44):1803272. doi:10.1002/adfm.201803272.
48. Liu XX, Zhou AW, Pan T, Dou YB, Shao MF, Han JB, et al. Ultrahigh-rate-capability of a layered double hydroxide supercapacitor based on a self-generated electrolyte reservoir. J Mater Chem. 2016;4(21):8421–7. doi:10.1039/C6TA02164F.
49. Hilal P, Fatma KD, Onses MS, Erkan Y, Ertugrul S. Outstanding supercapacitor performance with intertwined flower-like NiO/MnO_2/CNT electrodes. Mater Res Bull. 2022;149:111745. doi:10.1016/j.materresbull.2022.111745.
50. Mateen A, Javed M, Khan S, Saleem A, Majeed MK, Khan AJ, et al. Metal-organic framework-derived walnut-like hierarchical Co-O-nanosheets as an advanced binder-free electrode material for flexible supercapacitor. J Energy Storage. 2022;49:104150. doi:10.1016/j.est.2022.104150.
51. Seonghyun P, Byungseok S, Dongjoon S. Sodium-chloride-assisted synthesis of nitrogen-doped porous carbon shells via one-step combustion waves for supercapacitor electrodes. Chem Eng J. 2022;433:134486. doi:10.1016/j.cej.2021.134486.
52. Muhammad S, Azhar I, Ullah ZMS, Shah A, Asim S, Khan S, et al. Low-temperature synthesis of 3D copper selenide micro-flowers for high-performance supercapacitors. Mater Lett. 2022;314:131857. doi:10.1016/j.matlet.2022.131857.
53. Yu L, Shi NN, Liu Q, Wang J, Yang B, Wang B, et al. Facile synthesis of exfoliated Co-Al LDH-carbon nanotube composites with high performance as supercapacitor electrodes. Phys Chem Chem Phys. 2014;16:17936–42. doi:10.1039/C4CP02020K.
54. Zhang Y, Luo H, Zhang H. Polypyrrole nano-tube-interconnected NiCo-LDH nanocages derived by ZIF-67 for supercapacitors. ACS Appl Energy Mater. 2021;4:1189–98. doi:10.1021/acsaem.0c02465.
55. Yang YJ, Li W. Hierarchical Ni-Co double hydroxide nanosheets on reduced graphene oxide self-assembled on Ni foam for high-energy hybrid supercapacitors. J Alloys Comp. 2019;776:543–53. doi:10.1016/j.jallcom.2018.10.344.
56. Qiu TF, Luo B, Giersig M, Akinoglu EM, Hao L, Wang XJ, et al. Au@MnO_2 core-shell nanomesh electrodes for transparent flexible supercapacitors. Small. 2014;10:4136–41. doi:10.1002/smll.201401250.
57. Cai F, Kang YR, Chen HY, Chen MH, Li QW. Hierarchical CNT@$NiCo_2O_4$ core-shell hybrid nanostructure for high-performance supercapacitors. J Mater Chem. 2014;2(29):11509–15. doi:10.1039/C4TA01235F.
58. Zhao Y, Hu LF, Zhao SY, Wu LM. Asymmetric supercapacitors: preparation of $MnCo_2O_4$@$Ni(OH)_2$ core-shell flowers for asymmetric supercapacitor materials with ultrahigh specific capacitance. Adv Funct Mater. 2016;26:4085–93. doi:10.1002/adfm.201600494.
59. Yan AL, Wang WD, Chen WQ. The synthesis of $NiCo_2O_4$-MnO_2 core-shell nanowires by electrodeposition and its supercapacitive properties. Nanomaterials. 2019;9:1398. doi:10.3390/nano9101398.
60. Shao MF, Ning FY, Zhao YF. Core-shell layered double hydroxide microspheres with tunable interior architecture for supercapacitors. Chem Mater. 2012;24(6):1192–7. doi:10.1021/cm203831p.
61. Boorboor AF, Ostad M, Shahrak MN, Ershadi M, Malek SS, Ghasemi F, et al. Investigating MCM-41/Metal-Organic Framework nanocomposites as silicon-containing electrodes for supercapacitor. Surf Interfaces. 2022;29:101796. doi:10.1016/j.surfin.2022.101796.

62. Khan BA, Hussain R, Shah A, Mahmood A, Shah MZU, Ismail J, et al. $NiSe_2$ nanocrystals intercalated rGO sheets as a high-performance asymmetric supercapacitor electrode. Ceram Internat. 2022;48:5509–17. doi:10.1016/j.ceramint.2021.11.095.
63. Kannan RR, Lenin N, Banu AA, Sivabharathy M. Electrochemical behavior of MnO_2/MWCNT nanocomposites for electrode material in supercapacitor. Mater Lett. 2022;314:131887. doi:10.1016/j.matlet.2022.131887.
64. Nady JE, Shokry A, Khalil M, Ebrahim S, Elshaer AM, Anas M. One-step electrodeposition of a polypyrrole/NiO nanocomposite as a supercapacitor electrode. Sci Rep. 2022;12:3611. doi:10.1038/s41598-022-07483-y.
65. Yang YF, Li L, Luo BX, Shao ML, Fu XQ. Decorating flower-like $Ni(OH)_2$ microspheres on biomass-derived porous carbons for solid-state asymmetric supercapacitors. Chem Select. 2021;6:5218–24. doi:10.1002/slct.202100462.
66. Al-Hamyd MA, Al-Asadi AS, Al-Mudhaffer MF. Preparation and characterization of zinc-aluminum layered doubled hydroxide/graphene nanosheets composite for supercapacitor electrode. Physica E Low-Dimens Syst Nanostruct. 2022;136:115005. doi:10.1016/j.physe.2021.115005.
67. Jing L, Xiang CL, Zou YJ, Hu XB, Chu HL, Qiu SJ, et al. Spacing graphene and Ni-Co layered double hydroxides with polypyrrole for high-performance supercapacitors. J Mat Sci Technol. 2020;55:190–7. doi:10.1016/j.jmst.2019.10.030.
68. Wang Y, Dou H, Wang J. Three-dimensional porous MXene/layered double hydroxide composite for high performance supercapacitors. J Power Sources. 2016;327:221–8. doi:10.1016/j.jpowsour.2016.07.062.
69. Zhang D, Cao J, Zhang X. NiMn layered double hydroxide nanosheets *in-situ* anchored on Ti_3C_2 MXene via chemical bonds for superior supercapacitors. ACS Appl Energy Mater. 2020;3:5949–64. doi:10.1021/acsaem.0c00863.
70. Li YL, Shan LN, Sui YW. Ultrathin Ni-Co LDH nanosheets grown on carbon fiber cloth via electrodeposition for high-performance supercapacitors. J Mater Sci Mater Electron. 2019;30:13360–70. doi:10.1007/s10854-019-01703-4.
71. Wu ZJ, Ma TT, Chen JD, Yang W, Zou HB, Chen SZ. Study on the assemble of ASC with $NiCo_2O_4$/nickel foam composite. New Chem Mat. 2020;48:91–5. doi:10.19817/j.cnki.issn1006-3536.2020.08.019.
72. Qi XY, Zhou QF, Cui MW, Yang YZ, Jiang HW, Kang LT. Capacitive performance of Zn-Ni hydroxide nano-sheet arrays on nickel foams via a mild chemical-bath deposition process. J Inorganic Mat. 2017;32:372–8. doi:10.15541/jim20160333.
73. Li JY, Zhang WL, Li TY, Guo LF, Li G. Preparation of electrode materials by anodizing oxidation of stainless steel and its electrochemical properties. Micronanoelect Technol. 2020;57:687–93.
74. Wang XL, Cheng Y, Qiao XY, Zhang D, Xia YK, Fan JX, et al. High-loading and high-performance NiMn layered double hydroxide nanosheets supported on nickel foam for supercapacitor via sodium dodecyl sulfonate intercalation. J Energy Storage. 2022;52:104834. doi:10.1016/j.est.2022.104834.
75. Xiao Y, Su D, Wang X. Layered double hydroxides with larger interlayer distance for enhanced pseudocapacitance. Sci China Mater. 2018;61:263–72. doi:10.1007/s40843-017-9138-1.
76. Lin YY, Xie XL, Wang X, Zhang B, Li CJ, Wang H, et al. Understanding the enhancement of electrochemical properties of NiCo layered double hydroxides via functional pillared effect: an insight into dual charge storage mechanisms. Electrochim Acta. 2017;246:406–14. doi:10.1016/j.electacta.2017.06.067.
77. Quan W, Xu YY, Wang YT, Meng SC, Jiang DL, Chen M. Hierarchically structured Co_3O_4@glucose-modified LDH architectures for high-performance supercapacitors. Appl Surf Sci. 2019;488:639–47. doi:10.1016/j.apsusc.2019.05.301.